

FITTING ON BACK PANEL OF A MILITARY CARRIAGE – THOMAS STEEL – MODERN TIMES – SWITZERLAND

Artefact name	Fitting on back panel of a military carriage
Authors	Marianne. Senn (EMPA, Dübendorf, Zurich, Switzerland) & Christian. Degryny (HE-Arc CR, Neuchâtel, Neuchâtel, Switzerland)
Url	/artefacts/512/

≡ The object



Fig. 1: Fitting on back panel of a military carriage (©Tarchini),

Credit HE-Arc CR.

≡ Description and visual observation

Description of the artefact	Fitting on back panel, first exposed outdoors, later indoors (Fig. 1). Uniform corrosion and pitting corrosion are visible.
Type of artefact	Military carriage
Origin	Swiss Army, Thun, Bern, Switzerland
Recovering date	Built by Konstruktions-Werkstätte, 1918
Chronology category	Modern Times
chronology tpq	1918 A.D. ▼
chronology taq	---- ▼
Chronology comment	1918
Burial conditions / environment	Outdoor to indoor atmosphere
Artefact location	Historical Swiss Army Material Foundation, Burgdorf, Bern
Owner	Historical Swiss Army Material Foundation, Burgdorf, Bern
Inv. number	n.a.
Recorded conservation data	Not conserved

Complementary information

Nothing to report.

Study area(s)



Credit HE-Arc CR.

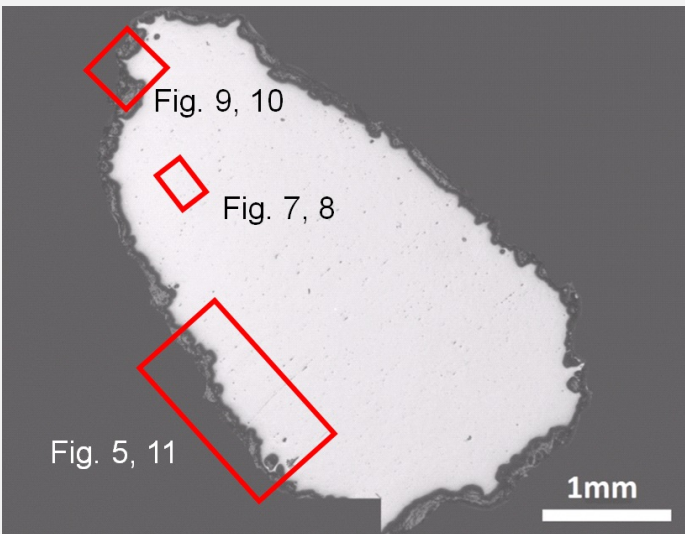
Fig. 2: Location of sampling area,

Binocular observation and representation of the corrosion structure

Stratigraphic representation: none.

MiCorr stratigraphy(ies) – Bi

Sample(s)



Credit HE-Arc CR.

Fig. 3: Micrograph of the cross-section of the sample taken from the fitting showing the location of Figs. 5 and 7 to 11,

Description of sample

	This sample is a cut from the corner of one of the two fittings on the back panel (Fig. 2). The metal is covered by a thin corrosion layer (Fig. 3).
Alloy	Thomas steel
Technology	Piled from several strips, hot rolled and annealed
Lab number of sample	POINT-Fe2
Sample location	Empa (Marianne Senn)
Responsible institution	Historical Swiss Army Material Foundation, Burgdorf, Bern
Date and aim of sampling	05/2009 metallography

Complementary information
Nothing to report.
✧ Analyses and results

Analyses performed: Metallography (nital etched after etching with Oberhoffer’s reagent), Vickers hardness testing, LA-ICP-MS, SEM/EDS.
--

✧ Non invasive analysis

✧ Metal

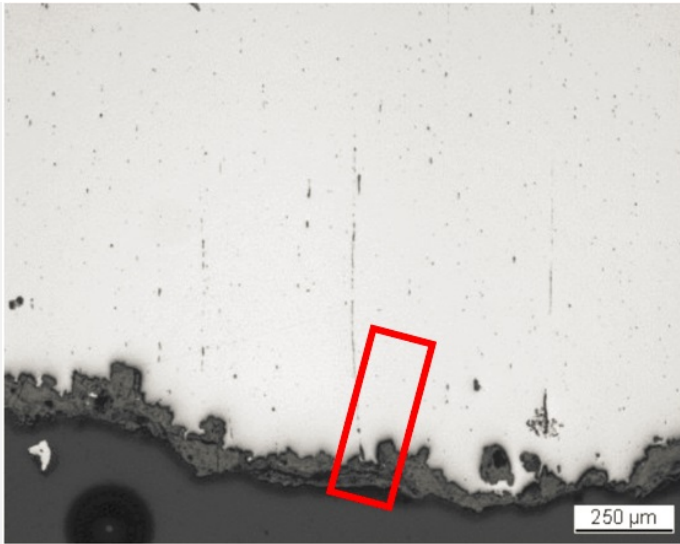
The remaining metal is a Mn-rich soft steel (C content around 0.1 mass%) containing manganese sulphide inclusions with a varying Fe content (Tables 1 and 2). The numerous inclusions form parallel rows (Fig. 5). This orientation is typical for hot rolled metal. After etching with Oberhoffer’s reagent, three main welding seams (P-rich) become visible (Fig. 6). Near the surface they are also outlined by corrosion (Figs. 5 and 11). After nital etching, the metal shows a ferritic structure with tertiary cementite and lamellar pearlite at the grain boundaries (Figs. 7 and 8). The grains are small with an ASTM grain size of 10 and are recrystallized due to annealing after hot rolling. The average hardness of the metal is HV1 165. The hardness is slightly high for such a structure and this is due to the Mn content of the metal. The chemical composition, especially the Mn content and the presence of carbo-nitrides (not analysed here), is typical for Thomas steel.

Elements	Ni/Co	Al	P	Ti	V	Cr	Mn	Co	Ni	Cu	As	Mo	Ag	Sn	Sb	W	C* mass%
Median (mg/kg)	2.4	<	300	<	<	140	3600	200	480	140	700	10	<	10	10	<	<0.1
Detection Limit (mg/kg)		5	82	10	2	13	2	1	3	1	3	3	1	1	1	4	
RSD %	1	-	8	-	-	3	7	2	1	6	3	7	-	7	8	-	

*visually estimated
Table 1: Chemical composition of the metal. Method of analysis: LA-ICP-MS. Lab Inorganic Chemistry, ETH.

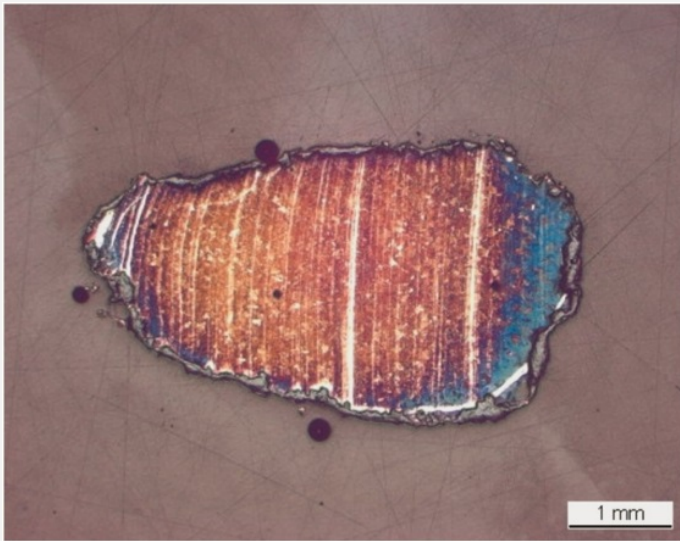
Elements	S	Mn	Fe	Cu	Total
Inclusions	26	46	31	2.2	105

Table 2: Chemical composition (mass %) of the inclusions. Method of analysis: SEM/EDS, Laboratory of Analytical Chemistry, Empa.



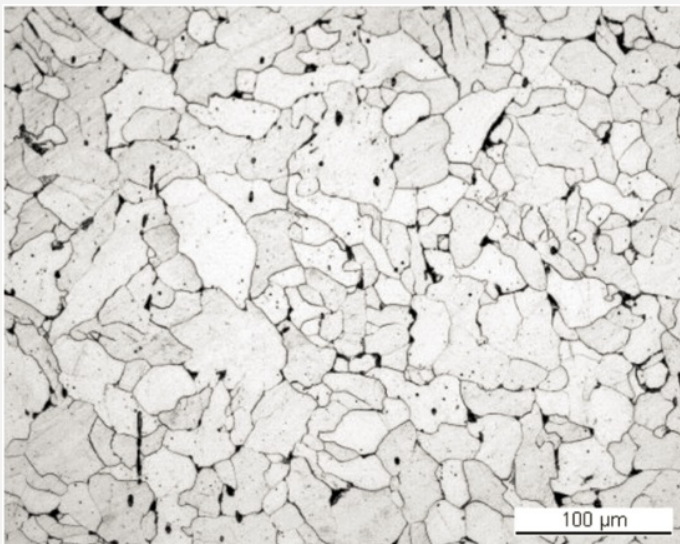
Credit HE-Arc CR.

Fig. 5: Micrograph of the metal sample from Fig. 3 (rotated by 270°, detail), unetched, bright field. We observe the metal including welding seams outlined by corrosion products and MnS inclusions. The area selected for elemental chemical distribution (Fig. 11) is marked by a red rectangle,



Credit HE-Arc CR.

Fig. 6: Micrograph of the metal sample from Fig. 3, etched with Oberhoffer's reagent, bright field. We observe three P-rich welding seams in white,



Credit HE-Arc CR.

Fig. 7: Micrograph of the metal sample, nital etched, bright field. We observe tertiary cementite (black) on the grain boundaries,

Fig. 8: SEM image of the metal sample from Fig. 3 (detail), BSE-mode, nital etched, bright field. The white ferrite grains contain lamellar pearlite (black arrow) and lenticular grey MnS inclusions (red arrow) in between the grain boundaries,



Credit HE-Arc CR.

Microstructure	Recrystallized grain structure with tertiary cementite
First metal element	Fe
Other metal elements	C, Mn

Complementary information

Nothing to report.

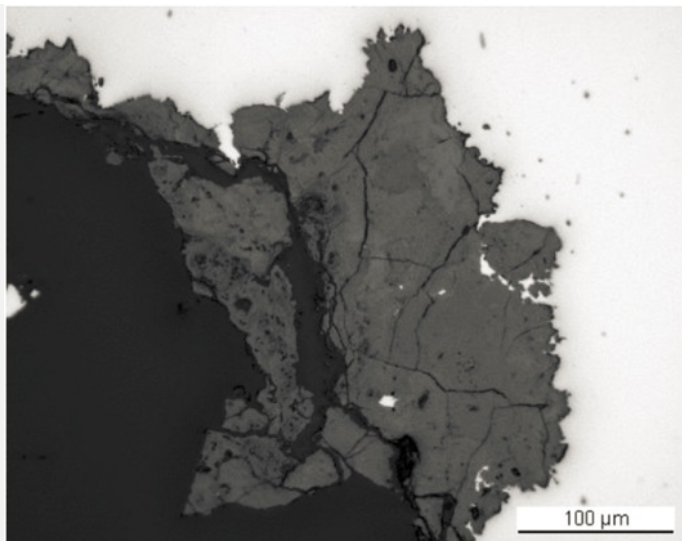
Corrosion layers

The average thickness of the corrosion products is about 80µm (Figs. 5 and 9). In bright field they appear grey, marbled and heavily cracked (Fig. 9). Under polarised light, the corrosion products appear orange to dark-brown (Fig. 10). At the metal - corrosion products interface they are dark-brown (CP3). The middle part (CP2) is red-orange and the outer part is bright orange (CP1). The elemental mapping of the corrosion layers shows no distinctive stratification, but areas near the metal - corrosion crust interface (CP3) as well as the top surface of the corrosion layer (CP1) seem to have a lower O content (Fig. 11). The O content indicates the presence of iron hydroxides (Table 3). Soil materials (such as rock fragments and dust) are found in the welding seams near the surface.

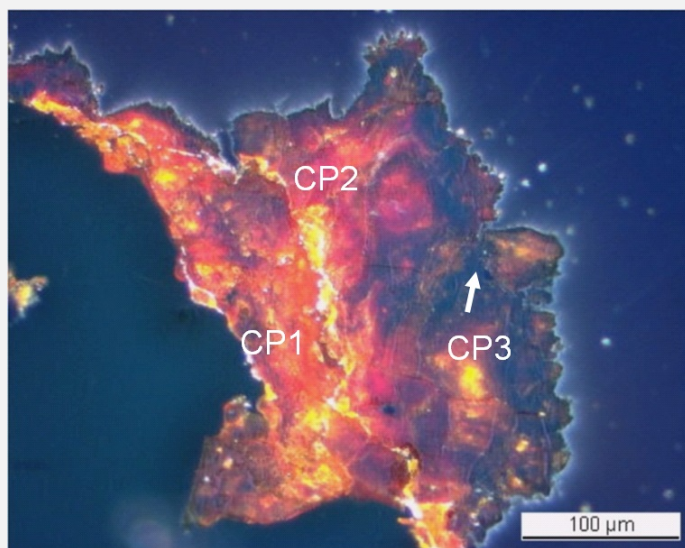
Location	Elements	O	S	Mn	Fe	Total
In welding seam		34	<	<	67	102
Inner corrosion layer (CP3)		38	0.7	0.8	66	106

Table 3: Chemical composition (mass %) of the corrosion layer (from Fig. 11). Method of analysis: SEM/EDS, Laboratory of Analytical Chemistry, Empa.

Fig. 9: Micrograph showing the metal - corrosion crust interface from Fig. 3 (rotated by 270°, detail), unetched, bright field. We observe in white the metal, in grey the corrosion products and in black the resin,

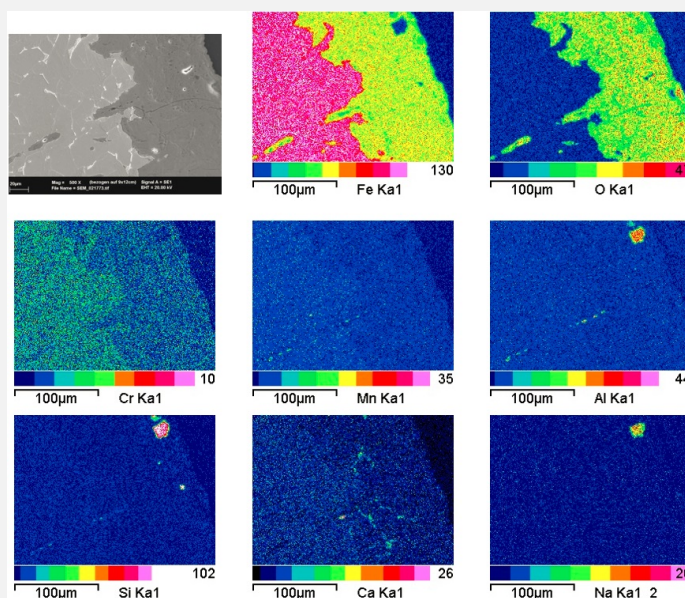


Credit HE-Arc CR.



Credit HE-Arc CR.

Fig. 10: Micrograph showing the metal - corrosion crust (same as Fig. 9) and corresponding to the stratigraphy of Fig. 4, unetched, polarised light. The corrosion products are dark-brown at the metal - corrosion crust interface and red-orange on the outside,



Credit HE-Arc CR.

Fig. 11: SEM image, BSE-mode, and elemental chemical distribution of the selected area from Fig. 5 (rotated by 270°, detail). Method of examination: SEM/EDS, Laboratory of Analytical Chemistry, Empa.

Corrosion form Uniform - transgranular

Corrosion type ?

Complementary information

Nothing to report.

✧ MiCorr stratigraphy(ies) – CS

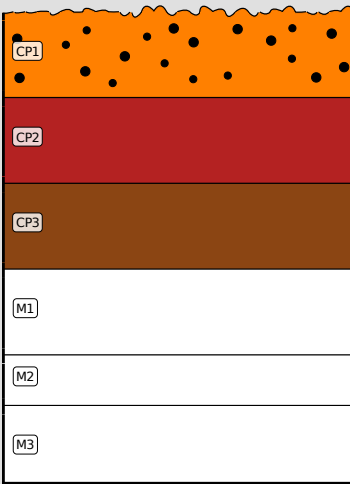


Fig. 4: Stratigraphic representation of the sample taken from the fitting in cross-section using the MiCorr application. The characteristics of the strata are only accessible by clicking on the drawing that redirects you to the search tool by stratigraphy representation. This representation showing for the metal part a welding seam (M2) can be compared to Fig. 10, Credit HE-Arc CR.

✧ Synthesis of the binocular / cross-section examination of the corrosion structure

Corrected stratigraphic representation: none.

✧ Conclusion

The fitting was produced from Mn-containing Thomas steel. It was forged out of four strips, hot rolled and annealed. The corrosion contains only few external markers such as sand grains and dust particles in the outermost layers. The presence of soil materials in the welding seams near the surface could be due either to the corrosion progress (by diffusion through the corrosion crust) or to the manufacturing process.

✧ References

<i>References on object and sample</i>
References object 1. Degriigny, C. (2011) Protection temporaire d’Objets métalliques base fer et cuivre à l’aide d’Inhibiteurs de corrosion Non Toxiques : application aux objets patrimoniaux techniques et scientifiques de grandes dimensions exposés en atmosphère non contrôlée, rapport interne HE Arc CR.
References sample 2. Rumo, L. (2009) Rapport Empa.
<i>References on analytic methods and interpretation</i>
ASTM E112-13: Standard Test Methods for Determining Average Grain Size.